Effect of metal catalyst on the mechanism of hydrogen spillover in three-dimensional covalent-organic frameworks*

Xiu-Ying Liu(刘秀英)[1], Jing-Xin Yu(于景新)[1], Xiao-Dong Li(李晓东)[1], Gui-Cheng Liu(刘桂成)[2,†], Xiao-Feng Li(李晓凤)[3], and Joong-Kee Lee[2]

[1] *College of Science, Henan University of Technology, Zhengzhou* 450000, *China*
[2] *Center for Energy Convergence Research, Green City Research Institute, Korea Institute of Science and Technology (KIST), Seoul* 02792, *Republic of Korea*
[3] *College of Physical and Electronic Information, Luoyang Normal University, Luoyang* 471022, *China*

(Received 7 October 2016; revised manuscript received 6 November 2016; published online 20 December 2016)

Hydrogen spillover mechanism of metal-supported covalent-organic frameworks COF-105 is investigated by means of the density functional theory, and the effects of metal catalysts M_4 (Pt_4, Pd_4, and Ni_4) on the whole spillover process are systematically analyzed. These three metal catalysts exhibit several similar phenomena: (i) they prefer to deposit on the tetra (4-dihydroxyborylphenyl) silane (TBPS) cluster with surface-contacted configuration; (ii) only the H atoms at the bridge site can migrate to 2,3,6,7,10,11-hexahydroxy triphenylene (HHTP) and TBPS surfaces, and the migration process is an endothermic reaction and not stable; (iii) the introduction of M_4 catalyst can greatly reduce the diffusion energy barrier of H atoms, which makes it easier for the H atoms to diffuse on the substrate surface. Differently, all of the H_2 molecules spontaneously dissociate into H atoms onto Pt_4 and Pd_4 clusters. However, the adsorbed H_2 molecules on Ni_4 cluster show two types of adsorption states: one activated state with stretched H–H bond length of 0.88 Å via the Kubas interaction and five dissociated states with separated hydrogen atoms. Among all the M_4 catalysts, the orders of the binding energy of M_4 deposited on the substrate and average chemisorption energy per H_2 molecule are $Pt_4 > Ni_4 > Pd_4$. On the contrary, the orders of the migration and diffusion barriers of H atoms are $Pt_4 < Ni_4 < Pd_4$, which indicates that Pt_4 is the most promising catalyst for the hydrogen spillover with the lowest migration and diffusion energy barriers. However, the migration of H atoms from Pt_4 toward the substrate is still endothermic. Thus direct migration of H atom from metal catalyst toward the substrate is thermodynamically unfavorable.

Keywords: covalent-organic frameworks, hydrogen spillover, hydrogen storage, density functional theory

PACS: 73.22.–f, 36.40.–c, 71.15.Mb **DOI:** 10.1088/1674-1056/26/2/027302

1. Introduction

Demand for energy sources is dramatically increasing with the rapid increase of population, while the traditional fossil energy is limited and the use of fossil energy leads to the emission of greenhouse gases.[1] This conflict has led to the increasingly urgent need for clean and ecologically friendly sources of energy.[2] Hydrogen has been regarded as a promising candidate due to its inherent advantages such as high energy density, clean, safe, sustainable, etc.[3] However, hydrogen storage remains one of the main challenges to the realization of fuel cell powered vehicles using hydrogen as an energy carrier.[4,5] Therefore, many different approaches and technologies for hydrogen storage have emerged, in which hydrogen storage on porous materials is one contender. Among various porous materials, covalent-organic framework (COF) is a class of highly porous material, because of its large surface area, extremely low density and porosity, hydrogen storage in COF has attracted significant attention since it was first synthesized in 2005.[6] It has been demonstrated that COF shows promising performances of hydrogen storage at very low temperatures.[7–9] However, its hydrogen uptake dramatically decreases at ambient temperature, due to the very weak van der Waals interactions between H_2 and COF (about 2 kJ/mol–5 kJ/mol),[10] which cannot satisfy the requirements for practical applications. It is worth remembering that the binding energy for the hydrogen storage system at moderate conditions (−30 °C–80 °C and 1 bar–100 bar, 1 bar = 10^5 Pa) should be 9.6 kJ/mol–58 kJ/mol to meet the requirements for practical applications.[11]

Hydrogen spillover has been experimentally demonstrated as an effective approach to improve the hydrogen storage properties of porous materials at room temperature, including activated carbons,[12] carbon nanotubes,[13] zeolites,[14] graphene,[15] and MOFs.[16] Hydrogen spillover is defined as the dissociative chemisorption of H_2 molecules on metal catalysts, the H migration onto adjacent surfaces

*Project supported by the National Natural Science Foundation of China (Grant Nos. 11304079, 11304140, 11404094, and 11504088), the China National Scholarship Foundation (Grant No. 201508410255), the Foundation for Young Core Teachers of Higher Education Institutions of Henan Province of China, the Foundation for Young Core Teachers of Henan University of Technology in China, the Korea Institute of Science and Technology (KIST) Institutional Program (Grant No. 2E26291) and Flag Program (Grant No. 2E26300), and the Research Grants of NRF funded by the National Research Foundation under the Ministry of Science, ICT & Future, Korea (Grant No. NRF-2015H1D3A1036078).

†Corresponding author. E-mail: log67@163.com

© 2017 Chinese Physical Society and IOP Publishing Ltd

of a receptor and the H diffusion on the substrate surface. Currently, hydrogen spillover has also been successfully applied to COFs.[17,18] For example, Li and Yang[17] studied the hydrogen storage of COF-1 by building carbon bridges, and found that the hydrogen uptakes were enhanced significantly by a factor of 2.6 at 298 K and 10 MPa. Kalidindi *et al.*[18] showed that the H_2 capacities were enhanced by a factor of 2–3 through Pd impregnation on COF-102 at room temperature and 20 bar.

Despite the fact that these promising results have been achieved, the plausibility of spillover mechanism and its usefulness as a hydrogen storage mechanism is still controversial. These controversies mainly arise from the limited understanding of the process that can be afforded through experiment.[19] Theoretical computational work can be very useful in this case. Therefore, many theoretical investigations have also been done on hydrogen spillover in COFs.[8,9,20–22] For example, Suri *et al.*[20] and Ganz and Dornfield[21] predicted the saturation hydrogen storage capacities of COF-1 and COF-5 by constructing the saturation models. However, the microscopic mechanism of improving the hydrogen storage performance was not involved. Ganz and Dornfield[22] further studied the thermodynamics and energetics of the initial stages of hydrogen spillover on the COF-5 material. They pointed out that spillover could not proceed on pure nor doped COF-5 because of high kinetic barrier. Our group[8] investigated molecular hydrogen and spillover hydrogen storage on several two-dimensional (2D) COFs, and found that their saturation densities were much larger than the physisorption uptakes of H_2 molecules at room temperature. Guo *et al.*[9] used the density functional theory (DFT) to study the hydrogen spillover mechanism of Pt_4 supported COFs. They pointed out that although the hydrogen storage capacity of COFs can be enhanced by spillover, due to the strong affinity of H atom on COFs surface, the high potential energy is required in the dissociation process. Therefore, it is necessary to discover other catalysts to reduce the migration and desorption barriers of H atoms.

Actually, the metal catalyst plays a very significant role in the spillover process; for example, to a great extent, it may determine whether the dissociation of H_2 molecules and migration of H atom toward the substrate can occur. Therefore, it is of great importance to study the effects of different metal catalysts on the entire spillover process in COFs, however, to our knowledge, such effects have not been reported to date. Currently, the most widely used metal catalysts in the spillover process are Ni, Pd, and Pt nanoparticles. Therefore, this paper aims to investigate the effects of different metal catalysts (Pt, Pd, and Ni) on hydrogen spillover mechanism and evaluate the feasibility of hydrogen spillover on the COF-105 via DFT calculations. We choose COF-105 as the model system because it is a typical three-dimensional (3D) COF with the highest hydrogen storage capacity among all the COFs, i.e., 21 wt% and 4.5 wt% at 77 K and room temperature with the pressure of 100 bar, respectively.[10] Herein, we mainly study the depositions of metal catalysts M_4 (Pt_4, Pd_4, and Ni_4) on COF-105, adsorptions and dissociations of H_2 molecules onto metal catalysts, H migrations from metal catalysts toward COF-105, and surface diffusion of H atom. The effects of Pt_4, Pd_4, and Ni_4 catalysts on each process are also compared with each other in detail.

2. Models and computational methods

2.1. Models

2,3,6,7,10,11-hexahydroxy triphenylene (HHTP) and tetra (4-dihydroxyboryl-phenyl) silane (TBPS) clusters were utilized to represent the building units constructing the COF-105 in order to reduce the computational cost, which were cut from the optimized periodic structure and terminated the breaking bonds with H atoms as shown in Figs. 1(a) and 1(b). For metal catalysts, we chose tetrahedral Pt_4, Pd_4, and Ni_4 clusters to present the corresponding nanoparticles, which are the smallest 3D clusters with sharp corners and edges that are considered as the most active catalytic sites. Although they are much smaller than real-sized catalysts, it has been shown that the size of the catalyst particles does not significantly affect H desorption energy at full saturation.[23] Therefore, using such a simplified cluster model can significantly reduce the computational cost, but still can reveal the intrinsic mechanism of spillover on metal supported COF-105 surface. The Pt_4, Pd_4, and Ni_4 clusters are shown in Figs. 1(c)–1(e).

2.2. Computational methods

All DFT calculations were carried out by using the Vienna ab initio simulation package (VASP)[24,25] with the exchange–correlation function of Perdew–Burke–Ernzerhof (PBE).[26] The core and valence electrons were described by projector augmented waves (PAW)[27] and a plane-wave basis set, respectively. An energy cutoff of 500 eV was used to make sure that the total energy is well converged. To avoid interactions between adjacent periodic images, the cluster models investigated in this paper were placed within a 25 Å×25 Å×25 Å box. The structural optimization was performed with the energy and force converging to less than 10^{-4} eV and 0.03 eV/Å, respectively. A 2×2×2 Monkhorst–Pack mesh was used to represent the Brillouin zone.

The Climbing Image Nudged Elastic Band (CI-NEB) method [28] was used to determine the minimum energy pathways of migration and diffusion of H atoms. All of the initial and final states were from optimized configurations. Six images between initial and final states were chosen to obtain smooth potential energy curves.

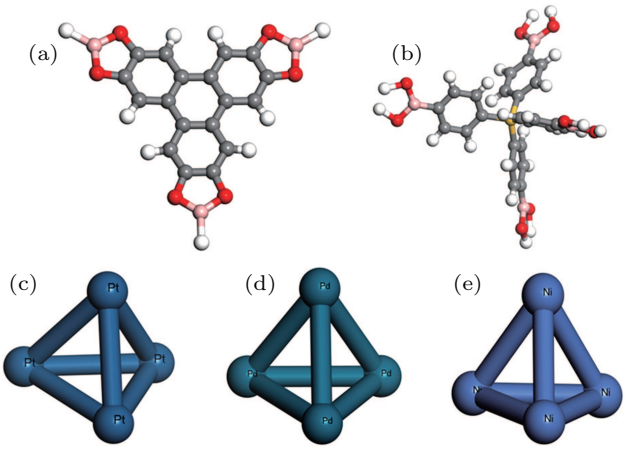


Fig. 1. (color online) Schematics of optimized HHTP (a), TBPS (b), Pt_4 (c), Pd_4 (d), and Ni_4 (e) clusters. Here, red, pink, gray, yellow, and white represent O, B, C, Si, and H, respectively.

3. Results and discussion

3.1. Metal catalysts deposited on HHTP and TBPS clusters of COF-105

First, we investigate how metal catalyst clusters M_4 (Pt_4, Pd_4, and Ni_4) are deposited on COF-105. Three deposition configurations are considered, which are point, edge and surface of M_4 contacting with HHTP and TBPS clusters, respectively. As a representative, the point, edge and surface deposition configurations of Pt_4 on HHTP and TBPS clusters are shown in Fig. 2. The binding energy of M_4 deposited on HHTP and TBPS is calculated as

$$\Delta E_{M_4} = E_{\text{substrate}} + E_{M_4} - E_{M_4@\text{substrate}}, \quad (1)$$

where $E_{\text{substrate}}$, E_{M_4}, and $E_{M_4\,@\text{substrate}}$ are the total energies of substrate, M_4 cluster, and M_4 deposited on the substrate, respectively.

The binding energies of point, edge and surface configurations of M_4 cluster on the substrate are listed in Table 1. It can be seen that for all the configurations of M_4 deposited on HHTP and TBPS clusters, the more the number of metal atoms contacting with the substrate, the larger the binding energy is. Concretely, the order of binding energies of the point, edge and surface configurations is cfg1<cfg2<cfg3, which indicates that the surface-contacted configuration is the most stable for M_4 deposited on the substrate. For all the M_4 clusters, the binding energies of M_4 on TBPS are larger than those on HHTP, which indicates that the interactions of TBPS with M_4 clusters are stronger than those of HHTP with M_4 clusters. This is mainly because TBPS cluster is 3D tetrahedral structure, whereas HHTP cluster is 2D triangular structural unit. Thus there are more C or B atoms interacting with metal atoms in the TBPS, resulting in the fact that the corresponding binding energies are larger than those of the HHTP.

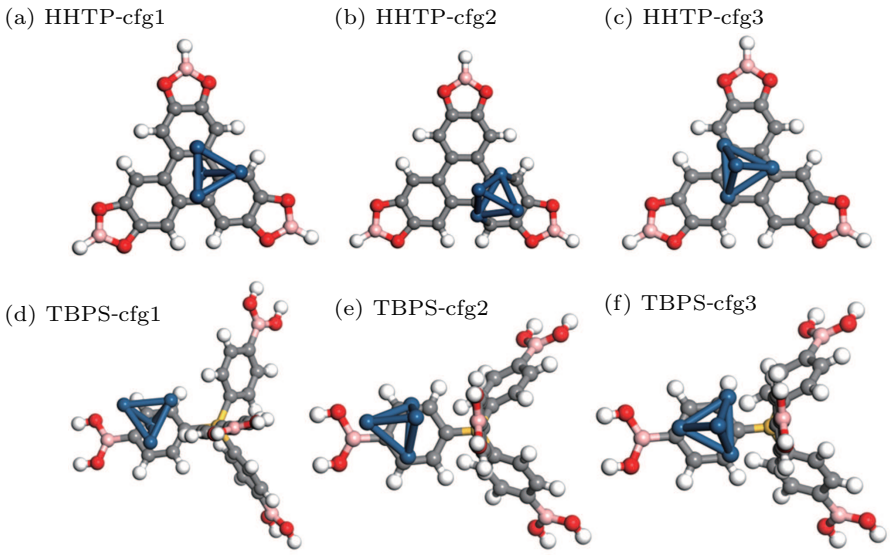


Fig. 2. (color online) Schematics of optimized deposition configurations of Pt_4 on HHTP and TBPS clusters, where cfg1, cfg2, and cfg3 represent point, edge, and surface configurations, respectively.

Table 1. Binding energies of different configurations of M_4 deposited on HHTP and TBPS clusters.

Configurations	ΔE_{M_4}/eV		ΔE_{M_4}/eV		ΔE_{M_4}/eV	
	Pt_4		Ni_4		Pd_4	
	HHTP	TBPS	HHTP	TBPS	HHTP	TBPS
Cfg1	1.65	2.26	1.26	1.92	0.53	1.69
Cfg2	1.74	2.43	1.58	2.18	0.90	1.88
Cfg3	1.88	2.57	1.79	2.34	1.29	2.04

The binding energies of M_4 on HHTP and TBPS are 1.65 eV–1.88 eV and 2.26 eV–2.57 eV for Pt_4, 1.26 eV–1.79 eV and 1.92 eV–2.34 eV for Ni_4, 0.53 eV–1.29 eV and 1.69 eV–2.04 eV for Pd_4, respectively, which indicates that among the interactions of Pt_4, Pd_4, and Ni_4 with the substrate, Pt_4 is the strongest, Ni_4 is the middle and Pd_4 is the weakest. This order is consistent with that of Sigal *et al.*[29] They used the DFT method to investigate the adsorption energies of hy-

drogen and oxygen on graphene decorated with a wide set of metals (Li, Na, K, Al, Ti, V, Ni, Cu, Pd, Pt). In conclusion, M_4 cluster is preferentially deposited in the vicinity of TBPS cluster and tend to be in the form of surface contact; Pt_4 and Pd_4 have the strongest and weakest interactions with the COF-105 surface, respectively.

3.2. Adsorption and dissociation of H_2 molecule on metal-catalyst-supported COF-105

In hydrogen spillover process, H_2 molecule first dissociates into H atoms around the metal catalyst through the interaction with metal catalyst, then the dissociated H atoms migrate toward the substrate and diffuse in the whole substrate surface. Thus the key conditions for hydrogen spillover to take place are as follows: 1) the H_2 molecules adsorbed onto metal catalyst can dissociate into H atoms; 2) the dissociated H atoms can overcome low energy barrier to migrate toward the COF-105 substrate; 3) H atoms can further diffuse in the COF-105 surface.

In this section, we consider the adsorption and dissociation of H_2 molecules on the M_4 catalyst. The saturated hydrogen adsorption configuration on the M_4 is the initial state of hydrogen spillover. Thus we successively place H_2 molecules in the vicinity of M_4 for M_4@substrate. Without the contact between M_4 and COF-105 surface after the optimization, up to 16 and 14 H atoms can be chemisorbed on Pt_4 for Pt_4@HHTP and Pt_4@TBPS, respectively, which indicates that the dissociation process of H_2 molecules is automatically to meet the first condition of hydrogen spillover. This result is consistent with that of Ref. [30]. The full H saturated adsorption configurations of Pt_4 for Pt_4@HHTP and Pt_4@TBPS are shown in Fig. 3. A similar phenomenon is also observed for the Pd_4 cluster. However, for the Ni_4 cluster, it would be saturated by six H_2 molecules for HHTP and TBPS clusters. The adsorbed H_2 molecules show two types of adsorption states:[31] an activated state with stretched H–H bond via the Kubas interaction and a dissociated state with separated hydrogen atoms. One activated state with H–H bond length of 0.88 Å exists on the top of the Ni atom. Another five H_2 molecules are dissociated into H atoms in the vicinity of N_4 cluster. The hydrogen saturated adsorption configurations of Ni_4 for Ni_4@HHTP and Ni@TBPS with surface contact configurations are shown in Fig. 4.

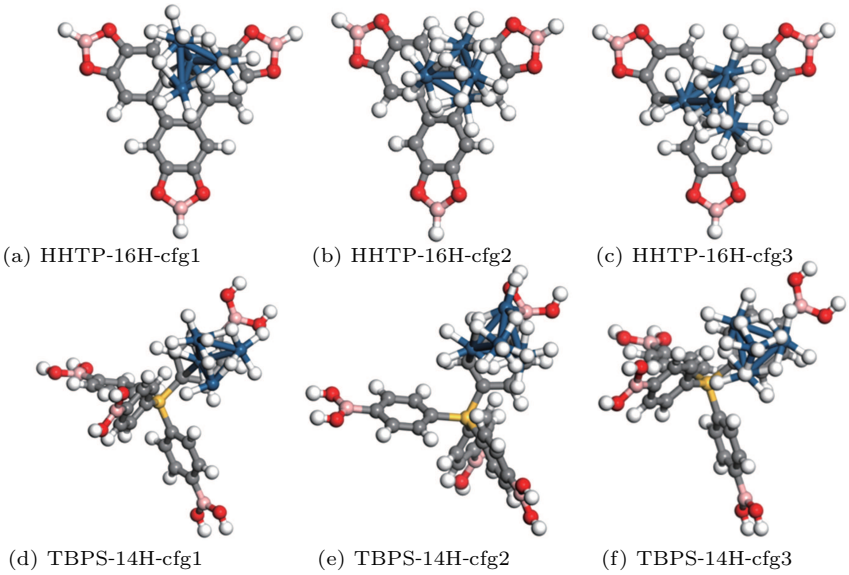


Fig. 3. (color online) Saturated hydrogen adsorption configurations on Pt_4 cluster for HHTP and TBPS with 16H and 14H atoms, respectively. Where all H_2 molecules are dissociated into H atoms, and cfg1, cfg2, and cfg3 represent point, edge, and surface configurations, respectively.

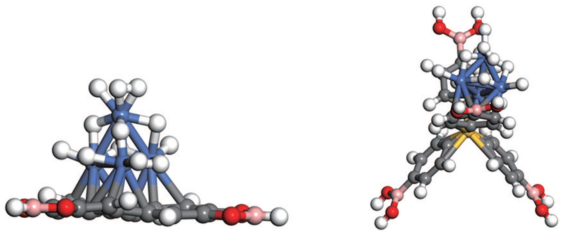


Fig. 4. (color online) Saturated hydrogen adsorption configurations on Ni_4 cluster for HHTP (a) and TBPS (b) clusters with surface contact configuration, where one activated state exists and another five H_2 molecules are dissociated into H atoms.

The average chemisorption energy of H_2 molecule on M_4 cluster is defined as

$$\Delta E_{\text{Chem}} = \frac{2[E_{M_4@\text{substrate}} + (n/2)E_{H_2} - E_{(n/2)H_2-M_4@\text{substrate}}]}{n}, \tag{2}$$

where $E_{M_4@\text{substrate}}$, E_{H_2}, $E_{(n/2)H_2-M_4@\text{substrate}}$, and n represent the total energies of bare M_4@ substrate, H_2 molecule, H saturated M_4@substrate, the number of H atoms on M_4 cluster, respectively.

The average chemisorption energy ΔE_{Chem} values of H_2

on M_4 clusters at full saturation with different configurations are obtained according to Eq. (2), which are listed in Table 2. For all the M_4@substrate clusters, the ΔE_{Chem} values of HHTP cluster are larger than those of TBPS cluster, which is contrary to the binding energies of M_4 deposited on the substrate. This indicates that the stronger the interaction of M_4 cluster with the substrate, the weaker the corresponding interaction of M_4 with H atoms is. It can also be seen that the greater the number of metal atoms contacting with the substrate, the smaller the ΔE_{Chem} is. Specifically, the order of ΔE_{Chem} values for point, edge and surface configurations is cfg1>cfg2>cfg3. This means that the interaction of M_4 with hydrogen atoms on the surface contact configuration is the weakest compared with those on the point and edge configurations, which favors the migration of H atom toward the substrate.

Table 2. Average chemisorption energies of H_2 adsorbed on Pt_4, Pd_4, and Ni_4 in a saturated level.

Configurations	ΔE_{Chem}/(eV/H_2)		ΔE_{Chem}/(eV/H_2)		ΔE_{Chem}/(eV/H_2)	
	Pt_4		Ni_4		Pd_4	
	HHTP	TBPS	HHTP	TBPS	HHTP	TBPS
Cfg1	1.25	1.09	1.04	0.97	0.75	0.62
Cfg2	1.11	1.03	0.99	0.89	0.68	0.58
Cfg3	0.95	0.91	0.85	0.78	0.63	0.53

The effects of Pt_4, Pd_4, and Ni_4 on ΔE_{Chem} are also compared. It can be seen that from Table 2, the ΔE_{Chem} values of H_2 on the M_4 cluster for HHTP and TBPS in a saturated level are 0.95 eV/H_2–1.25 eV/H_2 and 0.91 eV/H_2–1.09 eV/H_2 for Pt_4, 0.85 eV/H_2–1.04 eV/H_2 and 0.78 eV/H_2–0.97 eV/H_2 for Ni_4, 0.63 eV/H_2–0.75 eV/H_2 and 0.53 eV/H_2–0.62 eV/H_2 for Pd_4, respectively. That is, the order of ΔE_{Chem} values is Pt_4 >Ni_4 >Pd_4, which is consistent with that in Ref. [29]. This indicates that the Pt_4 and Pd_4 have the strongest and weakest interactions with hydrogen, respectively. Therefore, it can be concluded that (i) the ΔE_{Chem} of HHTP are larger than those of TBPS for all the M_4@substrate; (ii) the surface contact configuration is favorable for migration of H atoms compared with the point and edge contact configurations; (iii) the order of ΔE_{Chem} values is Pt_4 >Ni_4 >Pd_4.

3.3. Migration of H atoms from metal cluster toward the COF-105 substrate

The migration process of H atoms from M_4 toward the substrate surface is well studied by using the CI-NEB method. The adsorption locations of H atoms on M_4 clusters can be divided into the top site (adsorption at the top of metal atom in the form of metal–H bond) and the bridge site (adsorption onto the metal–metal bond in the form of metal–H–metal bond). The results show that only the H atoms on the bridge site can migrate to the COF-105 surface. However, for the H atom on the top site, even if we dragged it onto the C atom in the substrate, it would rebind to the top site of M_4 after optimization. This is mainly because the interactions of metal atoms with the top H atoms are stronger than those with the bridged H atoms, thus the H atoms onto the top site do not migrate easily. Wu *et al.*[32] also found a similar phenomenon when they investigated the migration of H atom from Pt_4 clusters toward B-doped graphene surface. It is noted that, when the H atom located on the bridge site (labeled as 1) migrates to the substrate surface, the other H atom located on the top site (labeled as 2) will migrate to this bridge site, resulting in the migration proceeding continuously and satisfying the second condition of hydrogen spillover. Especially for the H atoms onto the Ni_4 cluster, the activated H_2 molecule will be further dissociated into H atoms (labeled as 3 and 4) (see the inserts in Figs. 5(b) and 5(e)) when the H atom on the bridge site migrates to the substrate.

As surface contact configuration is most stable for M_4 deposited on the substrate as discussed in Subsection 3.1, we take the cfg3 configuration for example, and use the CI-NEB method to study the minimum energy pathways of the migration of H atom from M_4 toward the HHTP and TBPS surface, as shown in Fig. 5. The initial state (IS), transition state (TS) and final state (FS) are also shown in Fig. 5. It can be seen that for all the M_4 catalysts, the migration barriers of H atom from M_4 toward TBPS are lower than those toward HHTP which indicates that the migration process of the former is easier to happen. It is consistent with the discussion in Subsection 3.2, that is, the binding interactions of M_4@TBPS with H atoms are weaker than those of M_4@HHTP with H atoms, thus the migration barriers required are correspondingly lower. For Pt_4 catalyst, the migration barrier of H atom toward HHTP is 1.85 eV, slightly lower than the value of 1.92 eV reported by Guo *et al.*,[9] which further validates the reliability of our results. The migration barriers of Ni_4 and Pd_4 catalysts are higher than that of Pt_4 catalyst, specifically, 1.92 eV and 1.45 eV for Ni_4, 2.03 eV and 1.65 eV for Pd_4 toward the HHTP and TBPS, respectively. Therefore, it can be concluded that Pt_4 is the most favorable for the migration of H atom toward the substrate. However, for all M_4 catalysts, although the H atoms on the bridge site may migrate to the substrate, such high energy barriers and reaction energies (1.56 eV and 0.96 eV for Pt_4, 1.09 eV and 1.04 eV for Ni_4, 1.65 eV and 1.45 eV for Pd_4 on HHTP and TBPS, respectively) indicate that the migration reaction is not favored thermodynamically nor kinetically and cannot occur in normal conditions to any significant extent. Therefore, the direct migration of H atom toward the substrate is thermodynamically unfavorable.

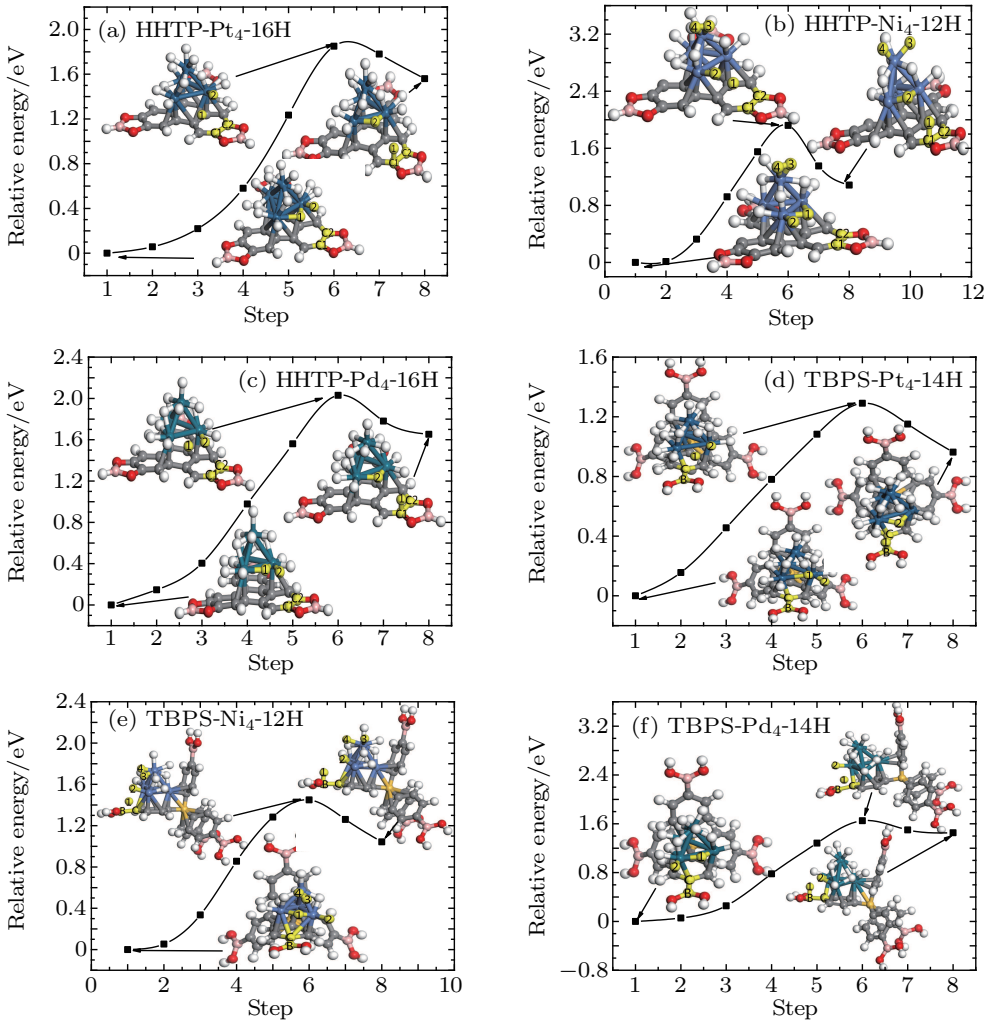


Fig. 5. (color online) Minimum migration energy pathways of H atoms from Pt_4, Pd_4, and Ni_4 catalysts toward the substrate, where the bridged H atoms migrate toward the C1 and B sites on HHTP and TBPS, respectively.

3.4. Diffusion of H atoms on the substrate surface

The diffusion processes of H atoms on M_4 supported and pure COF-105 surface are investigated, respectively. Their minimum diffusion pathways are shown in Fig. 6. The H diffusion barriers on the M_4 supported COF-105 surface are significantly reduced compared with those on the pure COF-105 surface, specifically, 0.66 eV and 0.43 eV for Pt_4, 0.78 eV and 0.51 eV for Ni_4, 0.91 eV and 0.65 eV for Pd_4 supported HHTP and TBPS, respectively. Whereas the corresponding diffusion barriers are 1.17 eV and 0.86 eV for HHTP and TBPS without M_4 catalyst, respectively. This indicates that the transition metal catalyst makes it easier for the diffusion process to occur. The diffusion barriers of H atoms on TBPS are lower than those on HHTP, resulting in the diffusion on the TBPS happening more easily, which is consistent with the discussion in the Subsections 3.2 and 3.3. In addition, for TBPS cluster, all of the diffusion reactions for Pt_4, Ni_4, and Pd_4 are exothermic, with the reaction energies of -0.26 eV, -0.16 eV, and -0.30 eV, respectively. However, the diffusion reaction is endothermic for Pd_4 supported HHTP substrate with a reaction energy of 0.21 eV, which remains thermodynamically unfavorable.

The effects of Pt_4, Ni_4, and Pd_4 catalysts on the diffusion process are also compared. As shown in Fig. 6, the diffusion barriers of H atom away from the vicinity of Pt_4 cluster are lowest, only 0.66 eV and 0.43 eV with the reaction energies of -0.10 eV and -0.26 eV on HHTP and TBPS, respectively, indicating that the diffusion process is exothermic. Therefore, Pt_4 catalyst is the most favorable for diffusion of H atom, which implies that a fast diffusion of H atoms on the COF-105 may happen under ambient conditions.

Combining the above discussion for the whole spillover process, we conclude the relationship between the metal catalyst and each step of spillover process. The binding energy of M_4 on the substrate ΔE_{M_4}, the average chemisorption energy per H_2 molecule ΔE_{Chem}, the migration barrier ΔE_M and diffusion barrier ΔE_D on the TBPS substrate for the surface-contacted configuration are shown in Fig. 7. The ΔE_{M_4} and ΔE_M are proportional to the ΔE_{Chem} and ΔE_D, respectively.

However, the ΔE_{M} and ΔE_{D} are inversely proportional to $\Delta E_{\mathrm{M_4}}$ and ΔE_{Chem}. Specifically, compared with Pd_4 and Ni_4 catalysts, Pt_4 has the largest $\Delta E_{\mathrm{M_4}}$, thus the largest ΔE_{Chem}, however, its ΔE_{M} and ΔE_{D} are correspondingly the lowest, which indicates that Pt_4 is the most favorable for hydrogen spillover on COF-105. However, the H migration process from Pt_4 toward the substrate is still endothermic. Therefore, other strategies should be explored for improving the thermodynamical feasibility, such as constructing a bridge between catalyst and substrate that is the main way used in the experiments. That is what we are going to do in the next step.

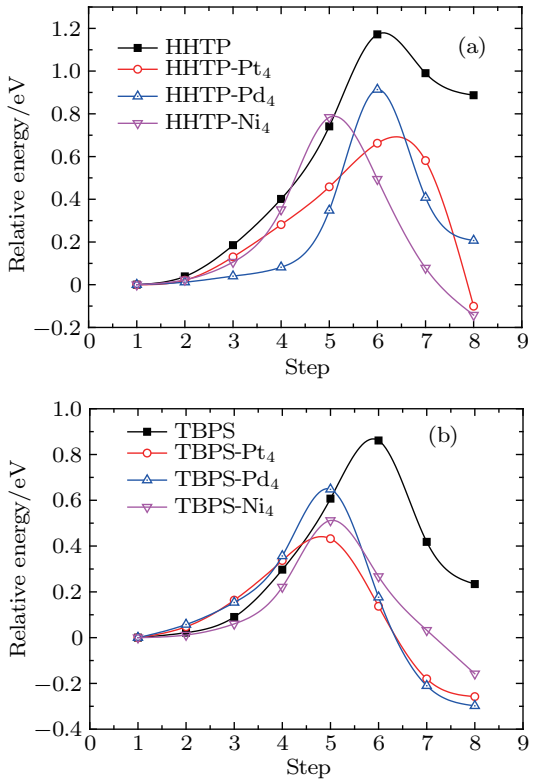


Fig. 6. (color online) Minimum diffusion energy pathways of H atoms on the COF-105 surface, where the diffusion pathways are along C_1 to C_2 path on HHTP (a) and B to C path on TBPS (b), respectively, which are labeled in the insets of Fig. 5.

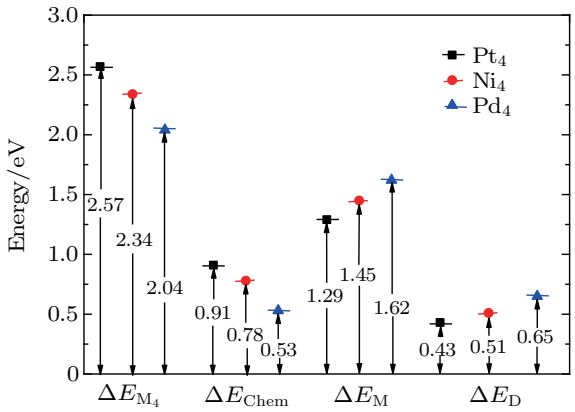


Fig. 7. (color online) Values of the binding energy $\Delta E_{\mathrm{M_4}}$, the average chemisorption energy per H_2 molecule ΔE_{Chem}, the migration barrier ΔE_{M}, and the diffusion barrier ΔE_{D} of Pt_4, Pd_4, and Ni_4 catalysts on the TBPS substrate for the surface-contacted configuration.

4. Conclusions

The hydrogen spillover mechanism on metal-supported COF-105 is investigated by DFT calculations, in which included mainly are various deposited configurations of metal catalyst on the COF-105, adsorption and dissociation of H_2 on the metal catalyst of M_4@COF-105 migration of H atoms from M_4 toward the COF-105 and diffusion of H atoms on the COF-105 surface. The results are shown as follows.

(I) The larger the number of metal atoms interacting with the substrate, the greater the binding energy of metal deposited on it will be. Metal catalyst prefers to deposit on TBPS cluster with surface contact configuration.

(II) Only H atoms located at the bridge site may migrate to the substrate surface, however, the migration process is an endothermic reaction and less stable.

(III) The introduction of metal catalyst can greatly reduce the diffusion energy barrier of H atoms on substrate surface, which makes it easier for the H atoms to diffuse on the substrate.

The effects of metal catalysts M_4 (Pt_4, Pd_4, and Ni_4) on the hydrogen spillover process have also been systematically compared. It is found that the order of binding energy of M_4 deposited on the substrate is Pt_4 >Ni_4 >Pd_4. The migration and diffusion barriers of H atom are lower for Pt_4 catalyst than those for Ni_4 and Pd_4 clusters, which indicates that Pt_4 is the most favorable for hydrogen spillover on COF-105. However, the H migration process from Pt_4 toward the substrate is still endothermic. Therefore, it is thermodynamically unfavorable that the H atoms directly migrate from metal catalyst toward the substrate. More efforts are needed to further improve the thermodynamical feasibility of hydrogen spillover, which is what we are going to do in the next step.

References

[1] Zhang F, Zhao P, Meng N and Maddy J 2016 *Int. J. Hydrogen Energy* **41** 14535
[2] Hu Y H 2013 *Int. J. Energy Res.* **37** 683
[3] Ruan W, Wu D L, Luo W L, Yu X G and Xie A D 2014 *Chin. Phys. B* **23** 023102
[4] Schlapbach L and Züttel A 2001 *Nature* **414** 353
[5] Liu X Y, Wang C Y, Tang Y J, Sun W G and Wu W D 2010 *Chin. Phys. B* **19** 036103
[6] Côté A P, Benin A I, Ockwig N W, O'Keeffe M, Matzger A J and Yaghi O M 2005 *Science* **310** 1166
[7] Spitler E L and Dichtel W R 2010 *Nat. Chem.* **2** 672
[8] Liu X Y, He J, Yu J X, Li Z X and Fan Z Q 2014 *Chin. Phys. B* **23** 067303
[9] Guo J H, Zhang H, Tang Y J and Cheng X L 2013 *Phys. Chem. Chem. Phys.* **15** 2873
[10] Klontzas E, Tylianakis E and Froudakis G E 2008 *J. Phys. Chem. C* **112** 9095
[11] Wong-Foy A G, Matzger A J and Yaghi O M 2006 *J. Am. Chem. Soc.* **128** 3494

[12] Lachawiec A J Jr, Qi G and Yang R T 2005 *Langmuir* **21** 11418
[13] Tsao C S, Liu Y, Chuang H Y, Tseng H H, Chen T Y, Chen C H, Yu M S, Li Q, Lueking A and Chen S H 2011 *J. Phys. Chem. Lett.* **2** 2322
[14] Lachawiec A J Jr and Yang R T 2008 *Langmuir* **24** 6159
[15] Pham V H, Dang T T, Singh K, Hur S H, Shin E W, Kim J S, Lee M A, Baeck S H and Chung J S 2013 *J. Mater. Chem. A* **1** 1070
[16] Li Y W and Yang R T 2006 *J. Am. Chem. Soc.* **128** 726
[17] Li Y W and Yang R T 2008 *AIChE J.* **54** 269
[18] Kalidindi S B, Oh H, Hirscher M, Esken D, Wiktor C, Turner S, Van Tendeloo G and Fischer R A 2012 *Chem. Eur. J.* **18** 10848
[19] Prins R 2012 *Chem. Soc.* **112** 2714
[20] Suri M, Dornfeld M and Ganz E 2009 *J. Chem. Phys.* **131** 174703
[21] Ganz E and Dornfeld M 2012 *J. Phys. Chem. C* **116** 3661
[22] Ganz E and Dornfeld M 2014 *J. Phys. Chem. C* **118** 5657
[23] Chen L, Cooper A C, Pez G P and Cheng H 2007 *J. Phys. Chem. C* **111** 5514
[24] Kresse G and Hafner J 1993 *Phys. Rev. B* **48** 13115
[25] Kresse G and Furthmüller J 1996 *Comput. Mater. Sci.* **6** 15
[26] Perdew J P, Burke K and Ernzerhof M 1996 *Phys. Rev. Lett.* **77** 3865
[27] Blöchl P E 1994 *Phys. Rev. B* **50** 17953
[28] Henkelman G, Uberuaga B P and Jónsson H 2000 *J. Chem. Phys.* **113** 9901
[29] Sigal A, Rojas M I and Leiva E P M 2011 *Phys. Rev. Lett.* **107** 158701
[30] Zhou C, Wu J, Nie A, Forrey R C, Tachibana A and Cheng H 2007 *J. Phys. Chem. C* **111** 12773
[31] Cabria I, López M J, Fraile S and Alonso J A 2012 *J. Phys. Chem. C* **116** 21179
[32] Wu H Y, Fan X F, Kuo J L and Deng W Q 2011 *J. Phys. Chem. C* **115** 9241